BIOCHEMISTRY
including biophysical chemistry & molecular biology

Article

pubs.acs.org/biochemistry

Role of the Surface-Exposed Leucine 155 in the Metal Ion Binding Loop of the CuA Domain of Cytochrome *c* Oxidase from *Thermus thermophilus* on the Function and Stability of the Protein

Manas Kumar Ghosh,[†] Jitumani Rajbongshi,[†,‡] Debajani Basumatary,[†] and Shyamalava Mazumdar*[,†]

[†]Department of Chemical Sciences, Tata Institute of Fundamental Research, Colaba, Mumbai 400005, India

[‡]Department of Chemistry, Gauhati University, Guwahati 781014, India

Supporting Information

ABSTRACT: The role of Leu155 in the metal ion binding loop in the soluble CuA binding domain of subunit II of cytochrome *c* oxidase from *Thermus thermophilus* (TtCuA) was investigated by site-specific mutations of this residue to arginine (L155R) and glutamic acid (L155E). The UV−visible absorption and electron paramagnetic resonance spectra suggested that the Cu_2S_2 core of TtCuA was almost unchanged by the mutations. The redox potential of the metal center in the L155R mutant was ∼20 mV higher than that in the WT protein, while that of the L155E mutant was almost the same as that of the wild type (WT-TtCuA). The rate of transfer of an electron from cytochrome c_{552} to the L155E mutant was much lower than that of transfer to the WT protein, while that for transfer to the L155R mutant was similar to that of WT-TtCuA. The total reorganization energy was increased for both the mutant proteins compared to WT-TtCuA. The results suggest that the presence of a negatively charged residue at the site of Leu155 in TtCuA possibly disfavors the protein−protein interaction between the two redox partners. The mutation also affected the equilibrium pH dependence of the protein. The thermal and thermodynamic stability of TtCuA was drastically decreased upon the mutation, which is most prominent in the L155R mutant. These studies indicate that the hydrophobic patch at the surface of TtCuA consisting of Leu155 is important for the transfer of an electron between cytochrome c_{552} and TtCuA.

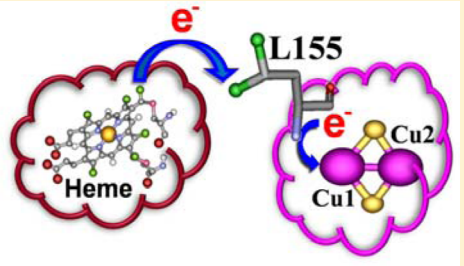

Cytochrome *c* oxidase is the terminal respiratory enzyme, which belongs to a heme copper oxidase superfamily. The purple dinuclear copper center (CuA) forms the electron entry site in cytochrome *c* oxidase (CcO).[1] The structure of the CuA site is highly conserved in subunit II of cytochrome *c* oxidases of eukaryotic mitochondria[2] and aerobic bacteria[3−6] and in nitrous oxide reductase of denitrifying bacteria.[7,8] This CuA site is a solvent-exposed part of subunit II of the enzyme and accepts electrons from cytochrome *c* and subsequently transfers the electrons to the binuclear heme a_3−CuB catalytic center through the heme *a* center in subunit I of the enzyme, leading to reduction of molecular oxygen to water at the binuclear catalytic center (Figure 1).[9] The structure of the CuA site shows the presence of a large number of *β*-sheets forming a *β*-barrel motif. Such extensive *β*-barrel cupredoxin topology of the CuA site was proposed to have a significant effect in adapting the specific coordination geometry of the dicopper center.[10,11] The solvent-exposed fragment obtained by truncating the first 44 residues of subunit II of CcO containing the CuA site from *Thermus thermophilus* is a soluble purple protein (TtCuA), which provides an excellent model for the electron entry site of the intact enzyme. TtCuA accepts the electron from cytochrome c_{552} (Ttc_{552}) that is involved in the electron transfer process in the terminal step of the bacterial respiratory system. The active site of Ttc_{552} consists of a low-spin iron(III) heme group axially coordinated to H15 and M69, with the heme group bound with thioether linkages to two cysteine residues in the protein matrix.[12,13]

The electron transfer reactions between proteins are essential for a large number of metabolic processes like photosynthesis, aerobic and anaerobic respiration, etc. The electron transfer complexes are usually transient protein−protein complexes, and the structures of only a few such complexes have been determined by X-ray crystallography.[14,15] Protein−protein docking simulations using the coordinates of individual proteins have been used to propose the probable electron transfer patch at the protein−protein interface.[16] The contact regions between WT-Ttc_{552} and WT-TtCuA were also estimated from $^{15}N-^{1}H$ TROSY [two-dimensional nuclear magnetic resonance (NMR)] studies in solution for each redox partner in the free state and in the complexed state. Experimental studies of intermolecular electron transfer using mutant proteins by techniques such as stopped-flow kinetics and NMR chemical shift mapping[16] can provide important information about the binding interface.

The crystal structure [Protein Data Bank (PDB) entry 2CuA (Figure 2)] shows that the two copper atoms are coordinated with two bridging cysteine residues (C149 and C153) forming

Received: May 2, 2011
Revised: February 28, 2012
Published: February 28, 2012

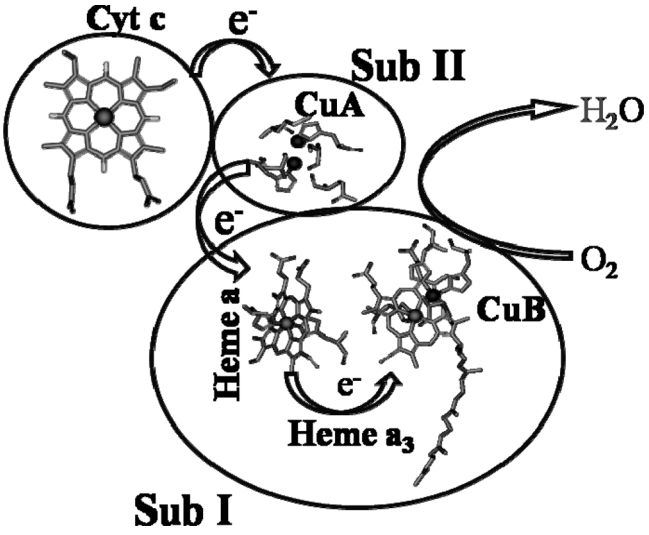

Figure 1. Schematic representation of the arrangement of functional subunits of *T. thermophilus* CcO and the metal active centers. The directions of electron flow and reduction of molecular oxygen to water are shown with arrows.

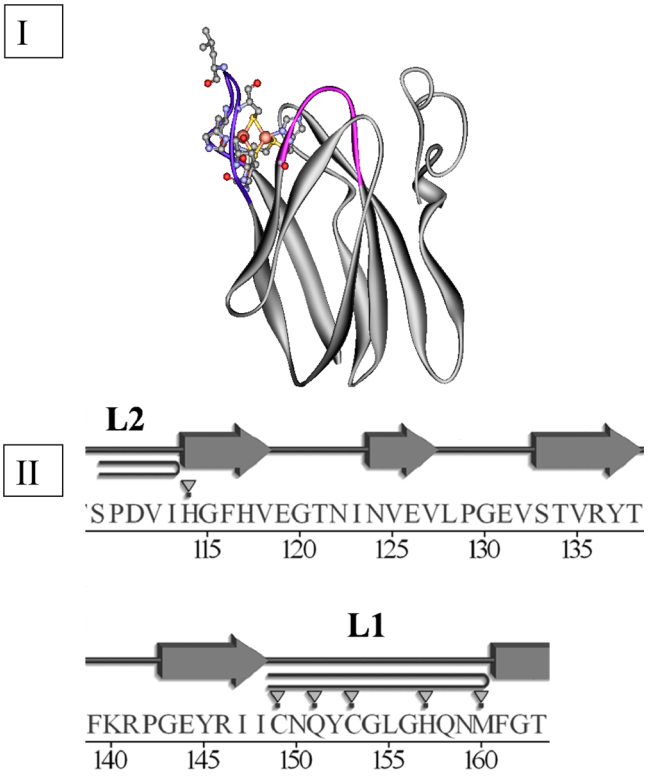

Figure 2. (I) Schematic structure of TtCuA (PDB entry 2CUA) showing Leu155 in the copper ion binding loops and the coordinating residues to the binuclear copper center. The copper binding loops are colored blue (L1) and magenta (L2). (II) Hairpin loops L1 and L2 in the secondary structure representation of part of the sequence of TtCuA.

the Cu_2S_2 core.[4] One of the copper ions (Cu1) is also coordinated with H157 and Q151, while the other copper ion (Cu2) is bound to H114 and M160. The binding site of the dinuclear copper center in the TtCuA is thus formed by residues 149−160 forming a hairpin loop (L1) between β-sheets 9 and 10 and one histidine residue (H114) from the hairpin loop (L2) between β-sheets 5 and 6 in the protein (Figure 2). Analyses of the sequence of the metal binding region of TtCuA indicated that apart from the residues that are coordinated to the metal ions, several residues in the metal binding loops (L1 and L2) are highly conserved. It is interesting that L155 is the only surface-exposed hydrophobic residue in loop L1 of TtCuA. Analyses of the sequence homology among CcO forms from various mammalian and bacterial sources, *Escherichia coli* ubiquinol oxidase, and nitric oxide reductase (N_2OR) showed that L155 is either invariant or replaced with a neutral or alcoholic residue in the homologous proteins. Understanding the specific structural and functional role of this residue in TtCuA is thus interesting.

This report describes the spectroscopic, kinetic, and electrochemical studies of the effect of site-specific mutation of L155 in TtCuA with arginine (L155R) and glutamic acid (L155E). We show that the replacement of a single amino acid residue led to a drastic decrease in the rate of intermolecular electron transfer in the L155E mutant. This mutant protein also showed a significantly increased energy of activation (E_a), enthalpy of activation ($\Delta H^{\ddagger}$), free energy of activation ($\Delta G^{\ddagger}$), and total reorganization energy (λ_T) for the transfer of an electron from its redox partner compared to those of the WT protein. The mutation of this surface-exposed residue was also shown to significantly affect the redox potential of TtCuA. The mutant proteins also showed a drastic decrease in thermal and thermodynamic stability. The TtCuA mutants also exhibited an altered pH-dependent conformational change in the metal center.

MATERIALS AND METHODS

Restriction enzymes and buffers for molecular biology were purchased from New England Biolabs. QuikChange site-directed mutagenesis kits were purchased from Stratagene. DEAE-Sepharose, CM-Sepharose, and Sephadex G-25 colo-umns were purchased from Pharmacia Biotech. General reagents were obtained from Sigma.

Mutation, Expression, and Purification. The wild-type CuA gene from *T. thermophilus* is inserted between NcoI and BamHI restriction sites in the pMA10 vector.[17] Site-directed mutagenesis was conducted using the QuikChange site-directed mutagenesis kit. The forward primers used for the mutation of leucine 155 to arginine and glutamic acid were 5′-CAGTACTGCGGCcgaGGCCACCAGAAC-3′ and 5′-GCAACCAGTACTGCGGCgaaGGCCACCAGAAC-3′, respectively, and the corresponding reverse primers were 5′-GTTCTGGTGGCCtcgGCCGCAGTACTG-3′ and 5′-GTTCTGGTGGCCttcGCCGCAGTACTGGTTGC-3′, respectively. The primers were purchased from Sigma Chemicals. These primers introduced BstzI and BlnI restriction sites into the *TtCuA* gene along with L155R and L155E mutations (shown in lowercase letters), respectively. Polymerase chain reaction (PCR) was conducted to amplify the mutant gene on a PTC-2000 Peltier thermocycler (MJ Research, Waltham, MA). Mutations were confirmed by restriction digestion as well as by DNA sequencing. The L155R and L155E mutants of TtCuA were overexpressed in *E. coli* (strain BL21-DE3) cells. Both the mutant proteins were purified according to the procedure reported previously.[17,18] Wild-type cytochrome c_{552} from *T. thermophilus* (WT-Ttc_{552}) was overexpressed in *E. coli* (strain JM109-DE3) cells containing the pET-22b(+)-c_{552} plasmid and cytochrome *c* maturation gene (pACYC-CCMO).[19] The protein was purified according to the procedure reported

dx.doi.org/10.1021/bi2017574 | *Biochemistry* 2012, 51, 2443−2452

previously.[19] The purity of the proteins was checked by sodium dodecyl sulfate−polyacrylamide gel electrophoresis. The purified proteins were stored at −20 °C in 20% glycerol, and aliquots of the proteins were filtered through PD10 (Pharmacia Biotech) columns to remove glycerol prior to further experiments.

UV−Visible Spectroscopy. UV−visible absorption spectra were recorded on a PerkinElmer Lambda 750 UV−vis spectrophotometer coupled with a Peltier-controlled thermostated cell holder. Optical absorption was monitored between 300 and 800 nm. All the optical absorption studies were conducted with protein concentrations in the range of 10−30 μM. The pH of the solutions were varied from 2 to 12 using the universal buffer [citric acid, potassium dihydrogen orthophosphate, disodium tetraborate, tris(hydroxymethyl)-aminomethane, and KCl], and the solutions were equilibrated at each pH for 48 h at room temperature for the study of the pH dependence of the L155R and L155E mutants of TtCuA.

Circular Dichroism Spectroscopy. Circular dichroism (CD) spectra were recorded on a JASCO J-810 spectropolarimeter equipped with a Peltier cell temperature controller. The CD spectra were recorded from 250 to 200 nm in a 0.1 cm path length quartz cell cuvette for the far-UV region and from 700 to 300 nm and in a 1 cm path length quartz cell cuvette for the visible region. The CD parameters were as follows: scan speed of 20 nm/min, time constant of 1.0 s, 1.0 bandwidth, and sensitivity of 100 mdeg. The CD spectra in the far-UV region (250−200 nm) were analyzed using Yang's method[20] to estimate the secondary structure of the protein. All experiments were conducted under a flow of pure nitrogen. A good signal-to-noise ratio in the CD spectra in this spectral range was obtained upon data averaging over three scans. Protein solutions (12 and 30 μM) were used for far-UV and visible CD studies, respectively.

EPR Spectroscopy. The X-band EPR spectra were recorded at 4 K on a Bruker 200D spectrometer with a microwave frequency of 9.42 GHz along with a continuous flow of helium cryostat. The temperature accuracy of the instrument is ±1 K. The concentration of the protein solution was 1 mM in 50 mM Tris buffer [tris(hydroxymethyl)aminomethane] (pH 6.5).

Electrochemistry. Voltammetric experiments were conducted at room temperature using an Autolab potentiostat-30 instrument in a three-electrode assembly with Ag/AgCl (3 M KCl) as the reference electrode, a platinum wire grid as the counter electrode, and glassy carbon (GC) as the working electrode. Nitrogen gas was purged through the solution for at least 10−15 min to remove any dissolved oxygen before every experiment. A nitrogen atmosphere was maintained over the solutions during the experiments. The electrode potential values were reported with respect to the normal hydrogen electrode (NHE). Prior to every experiment, suitable pretreatment of the working electrode was conducted. Pretreatment of the GC electrode involved polishing firmly on a microcloth using fine 0.05 μm alumina powders. It was then ultrasonicated for 2−3 min in Milli-Q water, rinsed thoroughly with Milli-Q water, and used immediately. The concentrations of proteins were 150 μM. Then, 60 μL of wild-type TtCuA and its mutants along with 0.1 M KCl was used for the experiment in a lab-made electrochemical micro cell setup analogous to that reported previously.[21]

Stopped-Flow Kinetics. Kinetic studies were conducted using a thermostated HI-TECH SCIENTIFIC SF-61 MX stopped-flow multimixing spectrofluorimeter. The sampling unit was mounted inside a thermostated bath compartment with the temperature varried (within ±1 °C) using a circulating water bath. The electron transfer kinetics of Ttc_{552} with mutants of TtCuA was investigated by mixing the different concentration of reduced Ttc_{552} with TtCuA. The stock solution of WT-Ttc_{552} (32 μM) in 50 mM Tris buffer (pH 7.0) was initially reduced in the stopped-flow syringe with 0.5 mM ascorbate anaerobically with a continuous flow of pure nitrogen gas. L155R and L155E mutants of TtCuA in 50 mM Tris (pH 7.0) were also made anaerobic by the passage of pure nitrogen gas. Pure nitrogen gas was purged through the solution for at least 10−15 min to remove any dissolved oxygen before every experiment. The solutions were mixed in the stopped-flow apparatus, and the time-dependent change in absorbance was followed at 552 nm. The temperature dependence of the electron transfer kinetics was monitored at different constant temperatures between 8 and 35 °C using a circulating water bath. The rate constants for the intermolecular electron transfer (k_{et}) between WT-Ttc_{552} and TtCuA variants were determined by plotting the observed rate constants as a function of ferrous WT-Ttc_{552} concentration at each temperature.

Thermal Unfolding. The temperature dependence of the visible CD was monitored to assess the thermal unfolding of the tertiary structures of the L155R and L155E mutants of TtCuA. The temperature was increased from 20 to 95 °C with a heating rate of 1 °C/min. The samples were equilibrated at each temperature for at least 3 min, and the reversibility of the unfolding was ensured by decreasing the temperature with a cooling rate of 1 °C/min.

Guanidine Hydrochloride (GuHCl)-Induced Unfolding. Visible CD was used to monitor the unfolding of the L155R and L155E mutants of the TtCuA by guanidine hydrochloride. Aliquots of the protein solution were equilibrated with various guanidine hydrochloride concentrations ranging from 0 to 7 M for 24−28 h at room temperature. The guanidine hydrochloride concentration was measured using a refractometer according to the reported procedure.[22]

Data Analysis. The time course of electron transfer between reduced Ttc_{552} and oxidized TtCuA (eq 1) was analyzed from the change in absorbance at 552 nm to determine the pseudo-first-order rate constant (k_{obs})

$$[Ttc_{552}]_{red} + [TtCuA]_{ox} \overset{k_{obs}}{\rightleftharpoons} [Ttc_{552}]_{ox} + [TtCuA]_{red} \quad (1)$$

The observed rate constant k_{obs} was plotted as a function of Ttc_{552} concentration to determine the rate constants for the intermolecular electron transfer (k_{et}) from Ttc_{552} to TtCuA.

The intermolecular electron transfer (k_{et}) rate constant was plotted as a function of the reciprocal of the temperature (T) to determine the energy of activation (E_a) of the proteins by the Arrhenius equation (eq 2).[23]

$$\ln k_{et} = -\frac{E_a}{RT} + \ln A \quad (2)$$

The thermodynamic parameters of activation such as the enthalpy of activation ($\Delta H^{\ddagger}$), the entropy of activation ($\Delta S^{\ddagger}$), and the free energy of activation ($\Delta G^{\ddagger}$) were determined by the Eyring equation (eqs 3 and 4) from the plot of the

logarithm of the k_{et}/T ratio as a function of the reciprocal of T.[23]

$$\ln \frac{k_{et}}{T} = -\frac{\Delta H^{\ddagger}}{RT} + \frac{\Delta S^{\ddagger}}{R} + \ln \frac{k_B}{h} \quad (3)$$

$$\Delta G^{\ddagger} = \Delta H^{\ddagger} - T\Delta S^{\ddagger} \quad (4)$$

The total reorganization energy (λ_T) of the proteins was calculated using the Marcus theory with the help of eq 5 assuming the value of λ_T is much greater than the driving potential (ΔG).[24]

$$\lambda_T = 4\Delta G^{\ddagger} - 2\Delta G \quad (5)$$

where $\Delta G = -nF\Delta E$, R is the universal gas constant, A is the pre-exponential factor, k_B and h are Boltzmann's constant and Planck's constant, respectively, ΔG is the Gibbs free energy, n is the number of electrons, F is the Faraday constant, and ΔE is the difference in reduction potentials of the two redox partner proteins.

The thermal unfolding data, monitored at different wavelengths, were analyzed using a two-state equilibrium model between native (N) and unfolded (U) conformations (N ⇌ U) to determine the different thermodynamic parameters such as ΔH_m, T_m, and ΔC_p for the unfolding transition.

The variation of ellipticity (θ_T^{λ}) with temperature at different wavelengths was analyzed using the generalized eq 6

$$\theta_T^{\lambda} = \theta_0^{\lambda} - 10C_0 l \times \frac{(\Theta_N^{\lambda} - \Theta_U^{\lambda})e^{-\Delta G_T/(RT)}}{1 + e^{-\Delta G_T/(RT)}} \quad (6)$$

where θ_0^{λ} is the CD value of the folded protein at wavelength λ at room temperature, C_0 is the protein concentration, and l is the length of the cuvette. Θ_N^{λ} and Θ_U^{λ} are the corresponding molar ellipticity coefficients of the folded and unfolded species at wavelength λ, respectively. T is the absolute temperature of the protein solution. The folding free energy, ΔG_T, at temperature T is related to the concentration of the denaturant guanidine hydrochloride, D, by linear free energy relationship[25] (eq 7)

$$\Delta G_T = \Delta G_T^0 - m_T D \quad (7)$$

where ΔG_T^0 is the free energy at 0 M guanidine hydrochloride at temperature T and m_T is the denaturant m value in the denaturant-induced unfolding at temperature T. The stability curves were obtained by plotting the values of ΔG_T^0 as a function of absolute temperature using the Gibbs−Helmholtz equation[18,19,25] (eq 8)

$$\Delta G_T^0 = \Delta H_m\left(1 - \frac{T}{T_m}\right) + \Delta C_p\left[T - T_m - T\ln\left(\frac{T}{T_m}\right)\right] \quad (8)$$

Different thermodynamic parameters such as ΔH_m, T_m, and ΔC_p were obtained from the analysis of the stability curves of the proteins. The maximal stability temperature (T_s) of the protein (eq 9) and the maximal folding free energy ($\Delta G_{T_s}^0$) of the protein were also determined from the stability curves.

$$T_s = T_m e^{(\Delta C_p - \Delta H_m/T_m - \Delta C_p \times T_m)/\Delta C_p} \quad (9)$$

Modeling Studies. Molecular modeling of the proteins was conducted using Discovery Studio Visualizer (Accelrys), and three-dimensional (3D) structures were compared using PDBeFold [Protein structure comparison service Fold at European Bioinformatics Institute (http://www.ebi.ac.uk/msd-srv/ssm), authored by E. Krissinel and K. Henrick].[26]

RESULTS AND DISCUSSION

UV−Visible Spectroscopy. The UV−visible absorption spectra of WT-TtCuA and its L155R and L155E mutants are similar to each other (Figure S1, Supporting Information). The absorption band at 360 nm was assigned to the (His)N → Cu interactions, and those at 477 and 530 nm were assigned to the Cys(S) → Cu charge transfer (CT) transitions in the Cu_2S_2 core.[27] The absorption band at 790 nm was assigned to the transition associated with the valence-delocalized CuA motif,[27] which remained almost unaffected on mutation (Figure S1, Supporting Information), indicating that the Cu_2S_2 core structure was retained in the mutants.

Circular Dichroism Spectroscopy. To study the effect of mutation on the conformational properties of the protein, we have conducted detailed CD studies of WT-TtCuA and its L155R and L155E mutants. The far-UV (190−260 nm) CD bands of the protein arise due to regular asymmetric structures, such as α-helix, β-sheet, turn, and random coils around the peptide bond. The secondary structure of the protein can be determined from the CD signal in the far-UV region. The results showed that the L155R and L155E mutations of TtCuA have no significant effect on the secondary structure of the protein (Figure S2, Supporting Information).

The specific coordination of the amino acids of the protein leads to an asymmetry in the electronic transitions of the Cu center that can be monitored by CD in the visible region (300−700 nm). The tertiary CD contains information about the spatial arrangements of the Cu ion and the aromatic side chains in the tertiary structure of the protein. Almost no change in the CD spectra (Figure S3, Supporting Information) of the protein was observed upon mutation of the Leu155 residue, indicating that the tertiary structure around the metal ion was possibly unaffected upon mutation of the residue in the loop region of the protein. Leucine is a nonpolar amino acid, whereas arginine and glutamate are polar amino acids; therefore, the mutation of this surface-exposed residue possibly affects the solvent microenvironment on the surface of the protein but does not alter the conformation around the metal ion.

EPR Spectroscopy. The EPR spectrum of WT-TtCuA is characterized by seven-line hyperfine splitting in the $g_{\perp}$ region corresponding to a valence-delocalized Cu_2S_2 configuration of the metal center.[18] Both the L155R and L155E mutants of TtCuA showed analogous EPR spectra with a $g_{\perp}$ of ∼2.00, a $g_{\parallel}$ of ∼2.18, and an $A_{\parallel}$ of ∼2.5 mT as reported previously for the WT protein (data not shown). The EPR results supported the idea that the valence-delocalized Cu_2S_2 core of TtCuA was not affected upon mutation of Leu155 to Arg (in L155R) or Glu (in L155E).

Redox Potentials. To determine whether the mutation of the Leu155 residue had any effect on the redox property of the protein, we conducted direct electrochemistry of the L155R and L155E mutants along with that of WT-TtCuA. The cyclic voltammograms of L155R and L155E along with that of WT-TtCuA are shown in Figure 3. Quasi reversible electrochemical responses with ΔE_P values of ∼60−80 mV were obtained on a glassy carbon electrode at an ambient pH of 6.5 for all the protein samples, supporting the idea that the metal ion is close to the surface of the protein and mutation of Leu155 does not

dx.doi.org/10.1021/bi2017574 | Biochemistry 2012, 51, 2443−2452

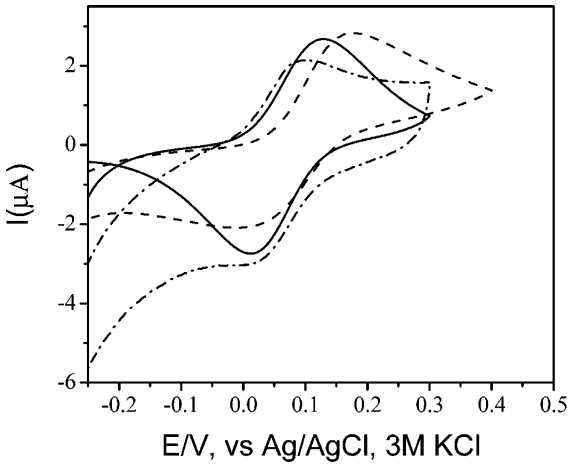

Figure 3. Cyclic voltammograms at a scan rate of 5 mV/s of WT-TtCuA (—), L155R TtCuA (---), and L155E TtCuA (–·–).

affect the electrode response of the protein. The apparent redox potentials (E_0) determined from electrochemistry were found to be 265 ± 10, 256 ± 10, and 285 ± 10 mV versus NHE for WT-TtCuA, the L155E mutant, and the L155R mutant, respectively. Plots of i_{pc} and i_{pa} versus the square root of the scan rate ($\sqrt{v}$) for WT-TtCuA and its L155R and L155E mutants yield straight lines (data not shown), which indicate a diffusion-controlled process.[28] The redox potential of Ttc_{552} is 200 mV as reported previously.[12]

The microenvironment of the active site has been altered by the mutation of positively and negatively charged amino acid residues arginine and glutamic acid, respectively. The hydrophobicity of the amino acid changed after mutation. The hydrophobicity was possibly involved in modulating the reduction potential of the metal center.

Intermolecular Electron Transfer by Stopped-Flow Kinetics. The transfer of electrons between WT-Ttc_{552} and the mutants of TtCuA was studied by stopped-flow kinetics. The absorbance at 552 nm decreased with time after reduced Ttc_{552} had been mixed with oxidized TtCuA, corresponding to reduction of the CuA center. The decrease in absorbance at 552 nm with time is shown in Figure 4. The decay curve was fit to a single-exponential equation to obtain the observed rate constant (k_{obs}), which was found to be linearly dependent on the concentration of Ttc_{552} while independent of TtCuA concentration in the range of our study. A linear fit to the observed rate constant (k_{obs}) versus the concentration of Ttc_{552} (Figure 5) gave the bimolecular electron transfer rate k_{et} as the slope of the line. The values of the intermolecular electron transfer rate (k_{et}) between Ttc_{552} and TtCuA were found to be (2.88 ± 0.05) × 10^6 M^{-1} s^{-1} for L155R and (1.14 ± 0.05) × 10^6 M^{-1} s^{-1} for L155E, while the rate of electron transfer for WT-TtCuA is (3.64 ± 0.05) × 10^6 M^{-1} s^{-1}. The rate of electron transfer for WT-TtCuA agreed well with that reported previously.[23] The rate of background reduction of TtCuA by sodium ascorbate used for reduction of Ttc_{552} was found to be very slow at pH 7, which agrees with earlier reports,[23,29,30] because of weak dissociation of ascorbic acid in solution. Therefore, as in an earlier report,[23] the observed electron transfer of WT-Ttc_{552} with L155R and L155E mutants of TtCuA was not affected by the presence of the ascorbate anion. The results thus clearly suggest that while mutation of Leu155 to Arg did not have any significant effect, the rate of transfer of an electron from WT-Ttc_{552} to the L155E mutant of TtCuA

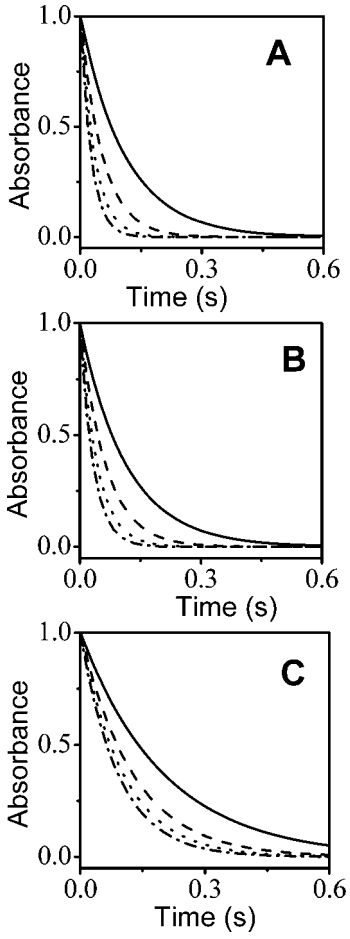

Figure 4. Plots of normalized absorbance at 552 nm vs time obtained by mixing 4 (—), 8 (---), 12 (···), and 16 μM (–·–) ascorbate-reduced WT-Ttc_{552} with 4 μM oxidized TtCuA variants in a stopped-flow setup at 8 °C: (A) WT-TtCuA, (B) L155R TtCuA, and (C) L155E TtCuA.

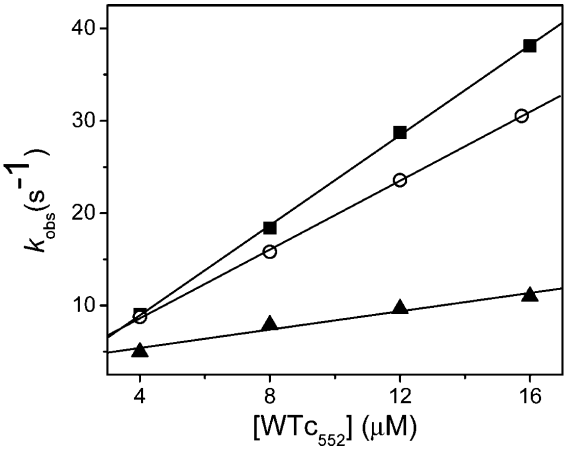

Figure 5. Plot of k_{obs} as a function of WT-Ttc_{552} concentration. The electron transfer reaction between ferrous WT-Ttc_{552} and oxidized (■) WT-TtCuA, (○) L155R TtCuA, and (▲) L155E TtCuA.

decreased by more than 3-fold compared to the rate of transfer to the WT-TtCuA at 8 °C.

The drastic decrease in the rate of transfer of an electron from Ttc_{552} to the L155E mutant of TtCuA compared to those of WT-TtCuA and the L155R mutant indicates that the presence of the negative charge at position 155 possibly

dx.doi.org/10.1021/bi2017574 | *Biochemistry* 2012, 51, 2443–2452

disfavors the protein−protein interaction between the two redox partners. Hairpin loop L1 [Figure 2 (residues 149−160)] consists of Cys, Asn, Gln, Tyr, Cys, and Gly on one side of Leu155 and Gly, His, Gln, Asn, and Met on the other side. Cys, His, Met, and one of the Gln residues (Q151) are coordinated to the copper ions, and Leu155 is the most surface-exposed residue in loop L1. It is interesting that a hydrophobic residue (Leu155) is stable on the surface of the protein though the protein is soluble in water. Comparison of the 3D structures (see Figure S4 of the Supporting Information) of the CuA binding site of TtCuA (PDB entry 2CuA) with that of the CuA binding site in subunit II of cytochrome *c* oxidase from *Paracoccus denitrificans* (PdCuA, PDB entry 1AR1B) showed[26,31] that Leu155 of TtCuA is at a position equivalent to Ile222 in PdCuA. Earlier studies[23,32,33] suggested that Trp121 in the cytochrome *c* oxidase of *P. denitrificans* may be involved in the transfer of an electron from cytochrome *c*, and this residue (Trp121) is close to Ile222 in PdCuA and forms a surface patch that may be involved in binding of cytochrome *c*. These results indicate that the surface patch consisting of Leu155 in TtCuA may thus have some important role in the biological function of cytochrome *c* oxidase of *T. thermophilus*. These results show that the transfer of an electron from reduced WT-Ttc_{552} to TtCuA was not much affected when Leu155 was replaced with the positive residue Arg (in L155R), while the rate was drastically decreased when a negative residue, Glu (in L155E), is present at this position. A negatively charged residue (Glu) in place of Leu155 seems to disturb the conformation of the protein−protein complex that is favorable for fast electron transfer between the two redox partners. The solution NMR structure of the complex of Ttc_{552} and TtCuA (PDB entry 2FWL) was reported on the basis of the topological description of the contact surface obtained by chemical shift analysis from the $^{15}N-^{1}H$ TROSY spectra of the individual proteins and of the mixture in solution. The NMR structures of the proposed protein−protein complex indicated that Leu155 of TtCuA is in the proximity of Thr117, Pro118, and Gln55 of Ttc_{552}.[16] Superposition of the NMR structure (PDB entry 2FWL) on the crystal structure of the intact enzyme (PDB entry 3EH3) indicated that there is a small change in the conformation of the L155 residue in the soluble fragment protein (TtCuA). Moreover, close inspection of the structure shows that the carbonyl of Leu155 may be hydrogen bonded (distance of 2.7 Å) to the terminal amide nitrogen of Gln55 of Ttc_{552}. Furthermore, the methyl side chains of Leu155 are only 3.1 Å from the β-carbon of Thr117 of Ttc_{552}, indicating possible hydrophobic contact in the complex (Figure 6). The earlier studies considered Ala87, Phe88, Arg146, Gly156, and Asn159 as the active residues for the interaction restraints in the docking analyses as they were most affected by the paramagnetic interactions of the heme.[16] Leu155, being located in the surface-exposed part of the loop (L1) between Gly156 and Asn159, might also be important in the formation of the transient complex between these two proteins.[16]

It is important to note that a previous study[34] of the isolated CuA fragment of cytochrome *c* oxidase from *P. denitrificans* had proposed that surface residues Q120 (Q148), E126 (E154), D178 (D206), D193 (D221), and E218 (E246) constitute the site of binding of cytochrome *c* to the soluble CuA protein. However, subsequent studies[35,36] of the intact cytochrome *c* oxidase (holoenzyme) showed that E126, D135, D159, and D178 of subunit II are instead involved in the electrostatic interaction with cytochrome *c* and W121 mediates the electron

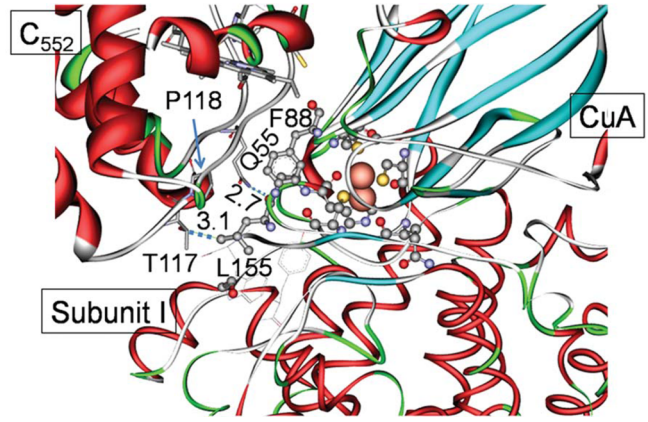

Figure 6. Schematic structure of the complex of cytochrome c_{552} with cytochrome *c* oxidase (CcO) from *T. thermophilus* obtained by superposing the NMR structure of the TtCuA−Ttc_{552} complex (PDB entry 2FWL) with the crystal structure of CcO (PDB entry 3EH3) showing the residues of cytochrome c_{552} (T117, P118, and Q55) interacting with L155 of CuA. The distances are given in angstroms. Red, cyan, and green signify α-helices, β-sheets, and coils, respectively.

transfer. Thus, the interaction of cytochrome *c* with the isolated soluble CuA protein[34] may be quite different from that in the case of the intact enzyme. These results about the significant role of L155 are based on the soluble fragment of subunit II (TtCuA) of the cytochrome *c* oxidase from *T. thermophilus*; hence, the role of L155 in the case of the intact holoenzyme cannot be unambiguously ascertained from these studies.

Reorganization Energy of the Proteins. The temperature dependence of the electron transfer reaction between Ttc_{552} and TtCuA is shown in Figure 7A. The data were fit to the Arrhenius equation (eq 2) to obtain E_a for the transfer of an electron from Ttc_{552} to TtCuA. Table 1 shows that the E_a values for WT-TtCuA and the L155R mutant were almost unchanged, but the L155E mutant showed a significant increase in the value $[\Delta E_a = E_a(\text{L155E}) - E_a(\text{WT}) = 2.9\ \text{kJ/mol}]$ of E_a compared to that for WT-TtCuA. The higher E_a in the L155E mutant suggests that there is an increase in the activation barrier for electron transfer. Analyses of the data according to the Eyring equation (eq 3) are shown in Figure 7B, which provide the thermodynamic activation parameters (Table 1). $\Delta H^{\ddagger}$ values of the WT and L155R mutant remain almost unchanged, but there is a significant increase $[\Delta\Delta H^{\ddagger} = \Delta H^{\ddagger}(\text{L155E}) - \Delta H^{\ddagger}(\text{WT}) = 3\ \text{kJ/mol}]$ in that of the L155E mutant. The $\Delta S^{\ddagger}$ values of the WT and mutant proteins remain almost unchanged. The total reorganization energy (λ_T) of the electron transfer process between the pair of proteins in this case was determined using the reported method.[24] The value of λ_T thus obtained is the sum of the reorganization energies of Ttc_{552} and TtCuA associated with the electron transfer process. The λ_T for the transfer of an electron from Ttc_{552} to WT-TtCuA is found to be 283.0 ± 0.3 kJ/mol at 298 K. A significant increase in the total reorganization energy was observed for both mutants (288.9 ± 0.3 kJ/mol for L155R and 292.0 ± 0.3 kJ/mol for L155E) of TtCuA. Assuming that the reorganization energy of Ttc_{552} remains unaffected, we can thus ascribe the increase in λ_T to the increase in the reorganization energy due to the mutation in the L155E and L155R mutants of TtCuA.

pH-Induced Conformational Change. As in the WT protein,[18] the UV−visible absorption spectra of the mutants of

dx.doi.org/10.1021/bi2017574 | *Biochemistry* 2012, 51, 2443−2452

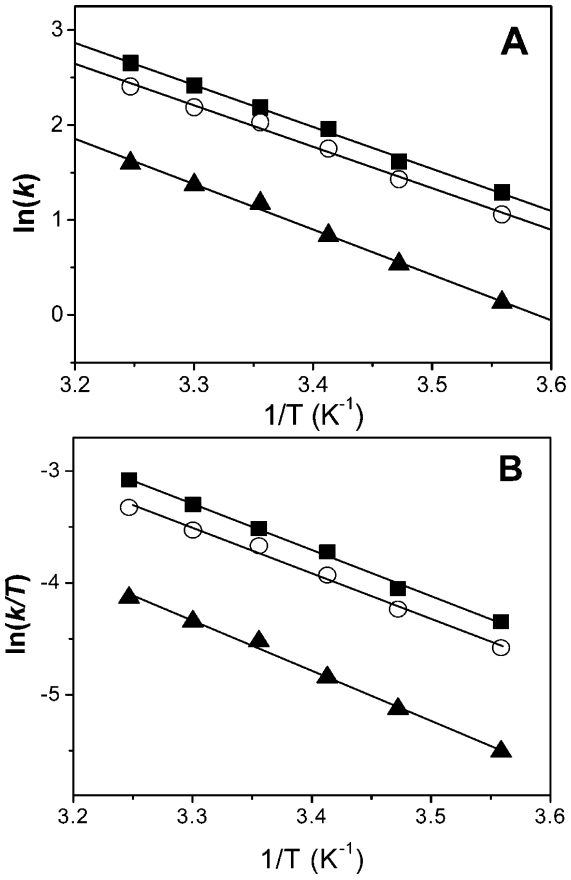

Figure 7. (A) Plot of the Arrhenius equation (eq 2) to obtain the energy of activation for the transfer of an electron between Ttc_{552} and TtCuA. The logarithm of the observed rate constants is plotted as a function of reciprocal temperature for the intermolecular electron transfer reaction between (■) Ttc_{552} and WT-TtCuA, (○) Ttc_{552} and L155R TtCuA, and (▲) Ttc_{552} and L155E TtCuA. (B) Plot of the Eyring equation (eq 3) to obtain the thermodynamic parameters of activation for the transfer of an electron between Ttc_{552} and TtCuA. The logarithm ratio of observed rate constants and temperature is plotted as a function of reciprocal temperature for the intermolecular electron transfer reaction between (■) Ttc_{552} and WT-TtCuA, (○) Ttc_{552} and L155R TtCuA, and (▲) Ttc_{552} and L155E TtCuA.

TtCuA show equilibrium changes at different pH values as shown in Figure 8 (see Figure S5 of the Supporting Information for the pH dependence of the spectra of the L155E mutant). The decrease in the absorbance of the bands at ~480, 530, and 790 nm with the increase in the absorbance at ~327 nm[17] with the increase in pH has been ascribed to the formation of a "valence-trapped" CuA center.[18] Plots of the absorbances of the visible absorption bands of the L155R and L155E mutants of TtCuA are shown in panels A and B of Figure S6 of the Supporting Information, which give apparent pK_a values of 8.0 for L155R and 10.2 for L155E. The apparent pK_a value for WT-TtCuA was reported to be 9.7.[18] The observed decrease in the apparent pK_a for L155R (pK_a = 8.0) compared to that of the WT protein (pK_a = 9.7) may be ascribed to the introduction of a positive charge (Arg residue in place of Leu) at the surface near the metal binding site that possibly disfavors the protonated form of certain amino acid(s) involved in the formation of the ligand environment around the Cu_2S_2 core in the protein. Analogously, the L155E mutant possibly introduces a negative charge at the surface that may favor the protonated form of certain residue(s) leading to an increase in the observed apparent pK_a to 10.2 of the mutant protein.

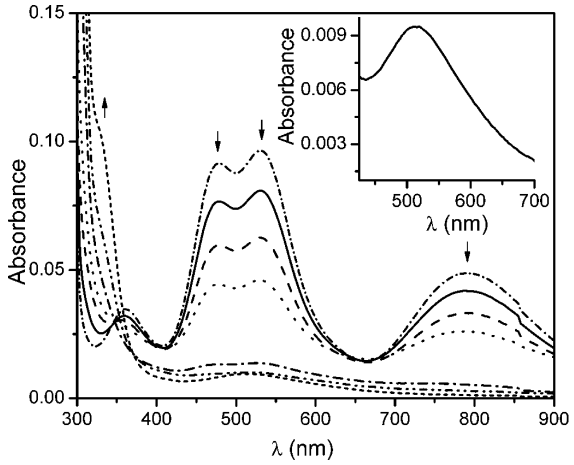

Figure 8. UV−visible absorption spectra of the L155R mutant of TtCuA from pH 6 to 12: pH 6 (···), pH 7 (---), pH 8 (−−−), pH 9 (···), pH 10 (−·−), pH 11 (−···), and pH 12 (—). The inset shows the 512 nm band of L155R at pH 12. The concentration of the protein solutions was 30 μM.

Unfolding of the L155R and L155E Mutants of TtCuA.

Thermal unfolding of the tertiary structure around the metal center in WT-TtCuA was shown to be incomplete even at 100 °C at ambient pH in the absence of any denaturant.[17,32,37] Mutation of the Leu155 residue to a charged residue was found to drastically decrease the thermostability of the protein. The apparent T_m values were found to be 70 and 97 °C for the L155R and L155E mutants, respectively. The values of ΔG_T^0 determined from the denaturant-dependent visible CD of the mutants were obtained at each temperature, and the stability curves of L155R and L155E mutants were constructed as shown in Figure 9. The stability curves show that the L155E mutant is both thermodynamically and thermally more stable than the L155R mutant of the protein, though both mutants have significantly low stability compared to that of WT-TtCuA.[17,32] The thermodynamic parameters for unfolding of the L155R and L155E mutants are listed in Table 2. The results showed that replacement of the surface-exposed Leu155 residue with a positive residue (Arg) leads to a decrease in the folding free energy of ~79 kJ/mol, while that with a negative residue (Glu) leads to a decrease of 66 kJ/mol compared to that of the WT protein at 20 °C. These changes in

Table 1. Activation Parameters for Intermolecular Electron Transfer between Ttc_{552} and TtCuA

protein	E_a (kJ/mol)	$\Delta H^{\ddagger}$ (kJ/mol)	$\Delta S^{\ddagger}$ (J mol^{-1} K^{-1})	$\Delta G^{\ddagger}$ (kJ/mol) at 298 K	λ_T (kJ/mol) at 298 K
WT-TtCuA	36.8 ± 0.5	34.3 ± 0.2	−112.0 ± 1.5	67.6 ± 0.2	283.0 ± 0.3
L155R TtCuA	36.3 ± 0.5	33.9 ± 0.2	−115.0 ± 1.5	68.1 ± 0.2	288.9 ± 0.3
L155E TtCuA	39.7 ± 0.5	37.3 ± 0.2	−111.0 ± 2.5	70.2 ± 0.5	292.0 ± 0.3

dx.doi.org/10.1021/bi2017574 | Biochemistry 2012, 51, 2443−2452

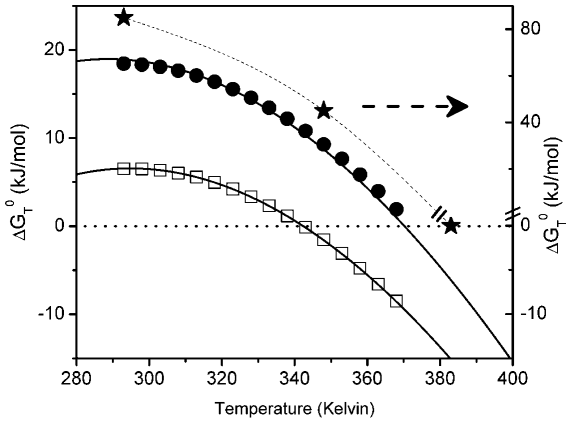

Figure 9. Protein stability curves plotted for the tertiary structure around the metal center of (★) WT-TtCuA, (□) L155R TtCuA, and (●) L155E TtCuA. Each point in the stability curves represents the free energy of unfolding (ΔG_T^0) at the corresponding temperature. The right arrow shows the vertical scale for the data for WT-TtCuA. The solid lines represent nonlinear curve fits to the Gibbs–Helmholtz equation using eq 8. The horizontal dotted line represents the zero free energy of unfolding. The data for WT-TtCuA were taken from refs 17 and 32.

the folding energy possibly arise from the changes in the solvent structure around the protein upon mutation.

CONCLUSIONS

The spectroscopic and electrochemical properties of the dinuclear CuA center of TtCuA provide direct information about subtle changes near the metal center in the protein. Mutation of the surface-exposed Leu155 in hairpin loop L1 of TtCuA by increased positive charge in the L155R mutant possibly favors the reduced form of the metal center and thereby increases the redox potential of the protein, while the redox potential of the L155E mutant of TtCuA remains almost the same as that of the WT protein. Mutation of Leu155 to Glu in TtCuA drastically decreased the rate of intermolecular electron transfer, which possibly suggests that the mutation may disturb the conformation of the protein–protein complex that is favorable for fast electron transfer between the two redox partners. The thermodynamic activation energy parameters and the total reorganization energy of the L155E mutant are significantly higher than those of the WT protein, indicating that the Leu155 residue might be a part of the surface patch involved in the interaction between Ttc_{552} and TtCuA. The introduction of a charged residue in place of the surface-exposed leucine in metal ion binding loop L1 affects the pH dependence of the conformational equilibrium between a "charge-delocalized" native form and a valence-trapped form of the metal center. The apparent pK_a was increased in the L155R mutant and decreased in the L155E mutant compared to that of the WT protein. Mutation of Leu155 affected the solvent interactions near the active site, which possibly had an important role in the decrease in the thermodynamic as well as the thermal stability of both mutants, with the effect being more prominent for the L155R mutant of TtCuA.

ASSOCIATED CONTENT

Supporting Information

UV–visible absorption spectra of WT, L155R, and L155E, far-UV CD spectra of WT, L155R, and L155E, visible CD spectra of WT, L155R, and L155E, the variation of absorbance as a function of pH for L155R and L155E, UV–visible absorption spectra of L155E mutants of TtCuA at different pH values, and 3D structural alignment using PDBeFold[26,31] for protein structure comparison of subunit II of CcO from *T. thermophilus* (TtCuA, PDB entry 2CuA) and that from *P. denitrificans* (PdCuA, PDB entry 1AR1B). This material is available free of charge via the Internet at http://pubs.acs.org.

Accession Codes

The coordinates and structure factors has been deposited in the Protein Data Bank as entries 2CuA (TtCuA), 1C52 (Ttc_{552}), 3EH3 (TtCcO), 2FWL (TtCuA–Ttc_{552} complex), and 1AR1B (PdCuA).

AUTHOR INFORMATION

Corresponding Author

*E-mail: shyamal@tifr.res.in. Telephone: +9122 22782363. Fax: +9122 22804610.

Funding

The work was supported by the Tata Institute of Fundamental Research (Mumbai, India).

Notes

The authors declare no competing financial interest.

ACKNOWLEDGMENTS

We thank Prof. B. Ludwig and Prof. Y. Watanabe for kindly providing us the plasmids and Mr. Sandeep Goyal and Mr. Saptaswa Sen for discussion and help. We also thank Mr. B. T. Kansara and Mr. Krishnendu Kundu for help.

ABBREVIATIONS

CcO, cytochrome *c* oxidase; TtCuA, CuA protein from subunit II of *T. thermophilus*; Ttc_{552}, cytochrome c_{552} from *T. thermophilus*; CD, circular dichroism spectroscopy; WT, wild type; L155R, leucine to arginine mutation at position 155; L155E, leucine to glutamic acid mutation at position 155; EPR, electron paramagnetic resonance; E_a, energy of activation; $\Delta H^{\ddagger}$, enthalpy of activation; $\Delta S^{\ddagger}$, entropy of activation; $\Delta G^{\ddagger}$, free energy of activation; λ_T, total reorganization energy.

Table 2. Thermodynamic Parameters for L155R and L155E Mutants of TtCuA[a]

protein	T_m (K)	T_s (K)	$\Delta G_{T_s}^0$ (kJ/mol)	ΔG_{293}^0 (kJ/mol)	ΔH_m (kJ/mol)
WT-TtCuA[b]	>373	–	–	85	(322)[c]
L155R TtCuA	343 ± 1	295 ± 1	6.7 ± 0.3	6.5 ± 0.3	92 ± 1
L155E TtCuA	370 ± 1	290 ± 1	18.9 ± 1	18.9 ± 1	165.6 ± 7.5

[a] T_m, T_s, $\Delta G_{T_s}^0$, ΔH_m, and ΔC_p were determined from nonlinear curve fitting of the respective protein stability curves using the Gibbs–Helmholtz equation. [b] Taken from ref 32. [c] For the reduced protein. The value for the oxidized protein would be higher than that for the reduced protein.

dx.doi.org/10.1021/bi2017574 | *Biochemistry* 2012, 51, 2443–2452

REFERENCES

(1) Chan, S. I., and Li, P. M. (1990) Cytochrome-c Oxidase: Understanding Natures Design of a Proton Pump. *Biochemistry 29*, 1−12.

(2) Tsukihara, T., Aoyama, H., Yamashita, E., Tomizaki, T., Yamaguchi, H., ShinzawaItoh, K., Nakashima, R., Yaono, R., and Yoshikawa, S. (1996) The whole structure of the 13-subunit oxidized cytochrome c oxidase at 2.8 angstrom. *Science 272*, 1136−1144.

(3) Wilmanns, M., Lappalainen, P., Kelly, M., SauerEriksson, E., and Saraste, M. (1995) Crystal structure of the membrane-exposed domain from a respiratory quinol oxidase complex with an engineered dinuclear copper center. *Proc. Natl. Acad. Sci. U.S.A. 92*, 11955−11959.

(4) Williams, P. A., Blackburn, N. J., Sanders, D., Bellamy, H., Stura, E. A., Fee, J. A., and McRee, D. E. (1999) The CuA domain of *Thermus thermophilus* ba3-type cytochrome c oxidase at 1.6 Å resolution. *Nat. Struct. Biol. 6*, 509−516.

(5) Ostermeier, C., Harrenga, A., Ermler, U., and Michel, H. (1997) Structure at 2.7 angstrom resolution of the *Paracoccus denitrificans* two-subunit cytochrome c oxidase complexed with an antibody F-V fragment. *Proc. Natl. Acad. Sci. U.S.A. 94*, 10547−10553.

(6) Iwata, S., Ostermeier, C., Ludwig, B., and Michel, H. (1995) Structure at 2.8-Angstrom Resolution of Cytochrome-c-Oxidase from *Paracoccus denitrificans*. *Nature 376*, 660−669.

(7) Brown, K., Tegoni, M., Prudencio, M., Pereira, A. S., Besson, S., Moura, J. J., Moura, I., and Cambillau, C. (2000) A novel type of catalytic copper cluster in nitrous oxide reductase. *Nat. Struct. Biol. 7*, 191−195.

(8) Haltia, T., Brown, K., Tegoni, M., Cambillau, C., Saraste, M., Mattila, K., and Djinovic-Carugo, K. (2003) Crystal structure of nitrous oxide reductase from *Paracoccus denitrificans* at 1.6 angstrom resolution. *Biochem. J. 369*, 77−88.

(9) Saraste, M. (1999) Oxidative phosphorylation at the fin de siecle. *Science 283*, 1488−1493.

(10) Wittung, P., Kallebring, B., and Malmstrom, B. G. (1994) The Cupredoxin Fold Is Found in the Soluble Cu-a and Cyoa Domains of 2 Terminal Oxidases. *FEBS Lett. 349*, 286−288.

(11) Holm, L., Saraste, M., and Wikstrom, M. (1987) Structural Models of the Redox Centers in Cytochrome-Oxidase. *EMBO J. 6*, 2819−2823.

(12) Fee, J. A., Chen, Y., Todaro, T. R., Bren, K. L., Patel, K. M., Hill, M. G., Gomez-Moran, E., Loehr, T. M., Ai, J. Y., Thony-Meyer, L., Williams, P. A., Stura, E., Sridhar, V., and McRee, D. E. (2000) Integrity of *Thermus thermophilus* cytochrome c(552) synthesized by *Escherichia coli* cells expressing the host-specific cytochrome c maturation genes, ccmABCDEFGH. Biochemical, spectral, and structural characterization of the recombinant protein. *Protein Sci. 9*, 2074−2084.

(13) Keightley, J. A., Sanders, D., Todaro, T. R., Pastuszyn, A., and Fee, J. A. (1998) Cloning and expression in *Escherichia coli* of the cytochrome c_{552} gene from *Thermus thermophilus* HB8: Evidence for genetic linkage to an ATP-binding cassette protein and initial characterization of the cycA gene products. *J. Biol. Chem. 273*, 12006−12016.

(14) Mathews, F. S., Sukumar, N., Chen, Z. W., Ferrari, D., Merli, A., Rossi, G. L., Bellamy, H. D., Chistoserdov, A., and Davidson, V. L. (2006) Crystal structure of an electron transfer complex between aromatic amine dehydrogenase and azurin from *Alcaligenes faecalis*. *Biochemistry 45*, 13500−13510.

(15) Dell'Acqua, S., Moura, I., Moura, J. J. G., and Pauleta, S. R. (2011) The electron transfer complex between nitrous oxide reductase and its electron donors. *J. Biol. Inorg. Chem. 16*, 1241−1254.

(16) Lucke, C., Muresanu, L., Pristovsek, P., Lohr, F., Maneg, O., Mukrasch, M. D., Rurterjans, H., and Ludwig, B. (2006) The Electron Transfer Complex between Cytochrome c_{552} and the Cu_A Domain of the *Thermus thermophilus* ba_3 Oxidase: A combined NMR and Computational Approach. *J. Biol. Chem. 281*, 14503−14513.

(17) Slutter, C. E., Sanders, D., Wittung, P., Malmstrom, B. G., Aasa, R., Richards, J. H., Gray, H. B., and Fee, J. A. (1996) Water-soluble, recombinant CuA-domain of the cytochrome ba3 subunit II from *Thermus thermophilus*. *Biochemistry 35*, 3387−3395.

(18) Sanghamitra, N. J., and Mazumdar, S. (2008) Conformational dynamics coupled to protonation equilibrium at the CuA site of *Thermus thermophilus*: Insights into the origin of thermostability. *Biochemistry 47*, 1309−1318.

(19) Nakajima, H., Ichikawa, Y., Satake, Y., Takatani, N., Manna, S. K., Rajbongshi, J., Mazumdar, S., and Watanabe, Y. (2008) Engineering of *Thermus thermophilus* Cytochrome c_{552}: Thermally Tolerant Artificial Peroxidase. *ChemBioChem 9*, 2954−2957.

(20) Yang, J. T., Wu, C. S. C., and Martinez, H. M. (1986) Calculation of Protein Conformation from Circular-Dichroism. *Methods Enzymol. 130*, 208−269.

(21) Hagen, W. R. (1989) Direct Electron-Transfer of Redox Proteins at the Bare Glassy-Carbon Electrode. *Eur. J. Biochem. 182*, 523−530.

(22) Ferreon, A. C., and Bolen, D. W. (2004) Thermodynamics of denaturant-induced unfolding of a protein that exhibits variable two-state denaturation. *Biochemistry 43*, 13357−13369.

(23) Maneg, O., Ludwig, B., and Malatesta, F. (2003) Different interaction modes of two cytochrome-c oxidase soluble CuA fragments with their substrates. *J. Biol. Chem. 278*, 46734−46740.

(24) Soriano, G. M., Cramer, W. A., and Krishtalik, L. I. (1997) Electrostatic effects on electron-transfer kinetics in the cytochrome f plastocyanin complex. *Biophys. J. 73*, 3265−3276.

(25) Pace, C. N., and Shaw, K. L. (2000) Linear extrapolation method of analyzing solvent denaturation curves. *Proteins Suppl. 4*, 1−7.

(26) Krissinel, E., and Henrick, K. (2004) Secondary-structure matching (SSM), a new tool for fast protein structure alignment in three dimensions. *Acta Crystallogr. D60*, 2256−2268.

(27) Gamelin, D. R., Randall, D. W., Hay, M. T., Houser, R. P., Mulder, T. C., Canters, G. W., de Vries, S., Tolman, W. B., Lu, Y., and Solomon, E. I. (1998) Spectroscopy of mixed-valence Cu-A-type centers: Ligand-field control of ground-state properties related to electron transfer. *J. Am. Chem. Soc. 120*, 5246−5263.

(28) Immoos, C., Hill, M. G., Sanders, D., Fee, J. A., Slutter, C. E., Richards, J. H., and Gray, H. B. (1996) Electrochemistry of the Cu-A domain of *Thermus thermophilus* cytochrome ba_3. *J. Biol. Inorg. Chem. 1*, 529−531.

(29) Alayash, A. I., and Wilson, M. T. (1979) Mechanism of Reduction of Single-Site Redox Proteins by Ascorbic-Acid. *Biochem. J. 177*, 641−648.

(30) Myer, Y. P., Thallam, K. K., and Pande, A. (1980) Kinetics of the Reduction of Horse Heart Ferricytochrome-c: Ascorbate Reduction in the Presence and Absence of Urea. *J. Biol. Chem. 255*, 9666−9673.

(31) Krissinel, E. (2007) On the relationship between sequence and structure similarities in proteomics. *Bioinformatics 23*, 717−723.

(32) Wittung-Stafshede, P., Malmstrom, B. G., Sanders, D., Fee, J. A., Winkler, J. R., and Gray, H. B. (1998) Effect of redox state on the folding free energy of a thermostable electron-transfer metalloprotein: The Cu-A domain of cytochrome oxidase from *Thermus thermophilus*. *Biochemistry 37*, 3172−3177.

(33) Flock, D., and Helms, V. (2002) Protein-protein docking of electron transfer complexes: Cytochrome c oxidase and cytochrome c. *Proteins: Struct., Funct., Genet. 47*, 75−85.

(34) Lappalainen, P., Watmough, N. J., Greenwood, C., and Saraste, M. (1995) Electron transfer between cytochrome c and the isolated CuA domain: Identification of substrate-binding residues in cytochrome c oxidase. *Biochemistry 34*, 5824−5830.

(35) Witt, H., Malatesta, F., Nicoletti, F., Brunori, M., and Ludwig, B. (1998) Tryptophan 121 of subunit II is the electron entry site to cytochrome-c oxidase in *Paracoccus denitrificans*: Involvement of a hydrophobic patch in the docking reaction. *J. Biol. Chem. 273*, 5132−5136.

(36) Witt, H., Malatesta, F., Nicoletti, F., Brunori, M., and Ludwig, B. (1998) Cytochrome-c-binding site on cytochrome oxidase in *Paracoccus denitrificans*. *Eur. J. Biochem. 251*, 367−373.

(37) Sujak, A., Sanghamitra, N. J., Maneg, O., Ludwig, B., and Mazumdar, S. (2007) Thermostability of proteins: Role of metal binding and pH on the stability of the dinuclear CuA site of *Thermus thermophilus*. *Biophys. J.* 93, 2845−2851.